Structural crossover from nonmodulated to long-period modulated tetragonal phase and anomalous change in ferroelectric properties in the lead-free piezoelectric $Na_{1/2}Bi_{1/2}TiO_3$-$BaTiO_3$

Badari Narayana Rao,[1] Dipak Kumar Khatua,[1] Rohini Garg,[1,2] Anatoliy Senyshyn,[3] and Rajeev Ranjan[1,*]

[1]*Department of Materials Engineering, Indian Institute of Science, Bangalore 560012, India*

[2]*Ceramics Division, Bhaba Atomic Research Center, Tromaby, Mumbai-400085, India*

[3]*Forschungs-Neutronenquelle Heinz Maier-Leibnitz (FRM II), Technische Universität München, Lichtenbergstrasse 1, D-85747 Garching b. München, Germany*

(Received 20 May 2015; revised manuscript received 8 June 2015; published 29 June 2015)

The highly complex structure-property interrelationship in the lead-free piezoelectric (x) $Na_{1/2}Bi_{1/2}TiO_3$ - ($1-x$) $BaTiO_3$ is a subject of considerable contemporary debate. Using comprehensive x-ray, neutron diffraction, dielectric, and ferroelectric studies, we have shown the existence of a new criticality in this system at $x = 0.80$, i.e., well within the conventional tetragonal phase field. This criticality manifests as a nonmonotonic variation of the tetragonality and coercivity and is shown to be associated with a crossover from a nonmodulated tetragonal phase (for $x < 0.8$) to a long-period modulated tetragonal phase (for $x > 0.80$). It is shown that the stabilization of long-period modulation introduces a characteristic depolarization temperature in the system. While differing qualitatively from the two-phase model often suggested for the critical compositions of this system, our results support the view with regard to the tendency in perovskites to stabilize long-period modulated structures as a result of complex interplay of antiferrodistortive modes [Bellaiche and Iniguez, Phys. Rev. B **88**, 014104 (2013); Prosandeev, Wang, Ren, Iniguez, ands Bellaiche, Adv. Funct. Mater. **23**, 234 (2013)].

DOI: 10.1103/PhysRevB.91.214116 PACS number(s): 77.80.Jk, 77.84.Cg, 61.05.fm, 77.80.bg

I. INTRODUCTION

The lead-free relaxor ferroelectric compound $Na_{1/2}Bi_{1/2}TiO_3$ (NBT) has been extensively investigated over the past six decades because of its highly complex and intriguing structure-property interrelationships. In the recent past, this compound has received considerable attention because certain chemical derivatives of NBT exhibit anomalous piezoelectric responses [1–3]. Although, similar to $Pb(Mg_{1/3}Nb_{2/3})O_3$ (PMN), NBT is categorized as a relaxor ferroelectric, there are notable differences with regard to the two systems. In contrast to PMN, NBT does not exhibit frequency dispersion of the dielectric maxima [4]. Further, unlike PMN, the thermal depolarization in NBT happens due to an intervening ferroelectric incompatible structural distortion comprising an in-phase octahedral tilt in the otherwise field stabilized structurally homogeneous rhombohedral state [5]. The diffuse scattering intensity does not exhibit anomalous rise on approaching T_m from the paraelectric side in NBT whereas it exhibits abrupt rise on approaching T_m in PMN [6]. Petzelt *et al.* [7] have recently compared the behavior of PMN and NBT from the lattice dynamical perspective. An obvious difference between PMN and NBT, which adds to the complications with regard to the understanding of the relaxor behavior of NBT *vis-à-vis* the PMN, is related to the fact that rhombohedral ground state in PMN emerges directly from the most symmetric cubic paraelectric phase, whereas the structure of the immediate paraelectric state of NBT is tetragonal $P4/mbm$ comprising in-phase tilted octahedra [8]. The absence of a group-subgroup relationship between the paraelectric tetragonal structure with an $a^0a^0c^+$ octahedral tilt and the ferroelectric rhombohedral structure with an $a^-a^-a^-$ octahedral tilt leads to atomic displacements taking a "tortuous" path while going from the paraelectric to the ferroelectric state. As a consequence, the structural state of the ferroelectric phase at room temperature of NBT carries the memory of its paraelectric state. Balagurov *et al.* [9] reported that the rhombohedral phase of NBT exhibits one-dimensional (1D) incommensurate modulation with a periodicity of ~6 nm along the fourfold axis of the precursor tetragonal phase. However, the authors postulated the existence of chemical ordering of Na and Bi on the A site to explain the 1D modulation. Local chemical ordering has earlier been invoked by Petzelt *et al.* [10] to explain soft infrared (IR) modes in the cubic phase of this compound. Though ordering of Na and Bi has been shown to be nonexistent in a recent scanning transmission electron microscopy (TEM) study using high-angle annular dark field imaging [11], using first principles computation, Groting *et al.* [12,13] have shown a correlation between the nature of chemical ordering and local structural distortion in NBT. The authors argued that because of comparable energies of the different types of local chemical ordering along with their octahedral tilt patterns, disordered NBT can be perceived as a mixed phase ground state with different average structures [13]. Rao *et al.* [14] have demonstrated that the high resolution synchrotron x-ray diffraction (XRD) pattern of NBT at room temperature can best be described in terms of the coexistence of monoclinic (Cc) and rhombohedral ($R3c$) phases and that the Cc structure vanishes after poling [14,15]. These results helped in the realization that the Cc global distortion reported by some groups [16,17] does not correspond to a new equilibrium phase but is rather a manifestation of the strain associated with local structural heterogeneities in the unpoled state [5,18]. Kreisel *et al.* [19] have suggested planar structural defects consisting of Bi cation off the [111] axis towards ⟨001⟩. Based on neutron pair distribution function studies, the local environments around Na and Bi have been reported to be different [20,21]. The distinctly different local environment

*rajeev@materials.iisc.ernet.in

of Bi^{+3} has been attributed to the bonding requirement of this ion to achieve a bond valence sum (BVS) close to its oxidation state [22]. Electron diffraction studies have revealed local in-phase ($a^0a^0c^+$) octahedral tilt embedded in the rhombohedral matrix [11,23].

In contrast to NBT, $BaTiO_3$ (BT) is a classical ferroelectric and exhibits sharp dielectric anomaly associated with the paraelectric-ferroelectric transition at ~130 °C. However, similar to classical relaxor ferroelectrics, BT exhibits considerable diffuse scattering corresponding to 1D ⟨001⟩ correlated atomic displacement [24,25]. Liu *et al.* [26] have reported the persistence of this 1D correlated chain in chemically modified BT exhibiting relaxor ferroelectricity, such as in Ba(Zr, Ti)O_3, Ba(Sn, Ti)O_3, and (Ba, Sr)TiO_3. The authors have argued that the role of substitutions is primarily to frustrate the transverse correlation between the 1D chain of correlated dipoles [26]. Recent first principles based effective Hamiltonian calculations have revealed that the polar nanoregions in Ba(Ti, Zr)O_3 are centered on Ti sites and that the dipole moments at the Zr sites are insignificant [27,28]. Though a similar kind of study has not been reported for A site substituted BT, Sr substitution has been reported to drive the system towards relaxor ferroelectricity [29]. Since NBT itself is a relaxor ferroelectric, it is anticipated that alloying of BT with NBT would also bring about a normal to relaxor transition above certain critical composition. However, unlike with the Sr substituted BT, the A site is substituted by two heterovalent ions Na^{+1} and Bi^{+3} in equal numbers in the NBT modified BT. As a result, both random electric fields and random strains would contribute to the formation of the domain state associated with the relaxor ferroelectricity [30,31].

The alloy system (x)NBT-$(1-x)$BT has been extensively investigated in the recent past because of its significance as a potential lead-free piezoelectric material. The majority of the studies have been reported for compositions around $x = 0.94$, which exhibit anomalous dielectric and piezoelectric response [32–38]. The first report by Takenaka *et al.* [36] suggested that the critical composition corresponds to a morphotropic phase boundary comprising the coexistence of tetragonal and rhombohedral phases in analogy with what is known for Pb(Zr, Ti)O_3. However, Ranjan and Dviwedi [37] reported a cubiclike structure and relaxor ferroelectric behavior for these compositions. Application of a strong electric field resulted in the cubic structure transformation to a rhombohedral and tetragonal phase mixture [34]. A recent neutron diffraction study of the critical compositions has revealed that the superlattice reflections cannot be indexed by the doubled pseudocubic cell suggested most often in the electron diffraction studies [37]. The BT end of this solid solution series has received less attention. Datta *et al.* [39] have reported a crossover from a first order to second order transition for x~0.20. In this paper, we have carried out a study of the (x)NBT-$(1-x)$BT system in the composition range $0.0 < x < 1.0$. This study revealed several interesting results, such as: (i) the crossover from the normal to relaxor behavior in the BT rich end is accompanied by an abrupt increase in the tetragonal distortion and Curie point; (ii) occurrence of the long-period modulation of the octahedral tilt suggesting the presence of competing tilt instabilities; and (iii) a strong correlation between the existence of long-period modulation of the octahedral tilt and appearance of a depolarization temperature before the dielectric maximum temperature (T_m).

II. EXPERIMENTAL PROCEDURE

Ceramic specimens of (x)NBT-$(1-x)$BT were prepared by the conventional solid state technique. Dried oxides of high purity Bi_2O_3 (99%; Sisco Research Laboratories Pvt. Ltd. [SRL]), Na_2CO_3 (99.9%; SRL), TiO_2 (99.8%; Alfa Aesar), and $BaCO_3$ (99%; SRL) were used as raw materials. Stoichiometric amounts of the oxides were mixed in a planetary ball mill for 10 h, using zirconia bowls and balls with acetone as the mixing medium. After drying, the mixed powders were calcined at 900 °C for 3 h in an alumina crucible. The calcined powders were then mixed with 2% polyvinyl alcohol (PVA) and pressed into pellets by uniaxial pressing at 150 MPa. These pellets were then sintered in air at 1200 °C for 2 h. Powder XRD patterns at room temperature and high temperature were collected from a Bruker powder diffractometer (model D8 Advance) using a Cu Kα x-ray source and nickel filter. Room temperature neutron powder diffraction data were collected using a wavelength of 1.548183 Å on the Structure Powder Diffractometer (SPODI) at the Forschungs-Neutronenquelle Heinz Maier-Leibnitz (FRM II) neutron reactor (Germany). Rietveld refinement was carried out using the FullProf package version 2000 [40]. A Precision Premier II tester (Radiant Technologies, Inc.) was used to obtain the polarization-electric (P-E) field hysteresis measurements. The dielectric measurements were carried out using a Novocontrol Alpha-A impedance analyzer.

III. RESULTS

A. Normal-relaxor ferroelectric crossover

Figure 1 shows the temperature variation of relative permittivity of $(1-x)BaTiO_3$-$(x)Na_{1/2}Bi_{1/2}TiO_3$ in the composition range $0.0 \leqslant x \leqslant 0.90$. As expected, the dielectric anomaly of BT is sharp and is representative of a ferroelectric-paraelectric transition. With increasing NBT concentration, the Curie point increases. However, the sharp dielectric anomaly in the real part turns to diffuse for $x > 0.20$, suggesting the setting in of the relaxor tendency. The frequency dependence of permittivity maximum temperature, however, was not clear in the real part of the permittivity data. This feature could be captured in the imaginary part of the dielectric permittivity,

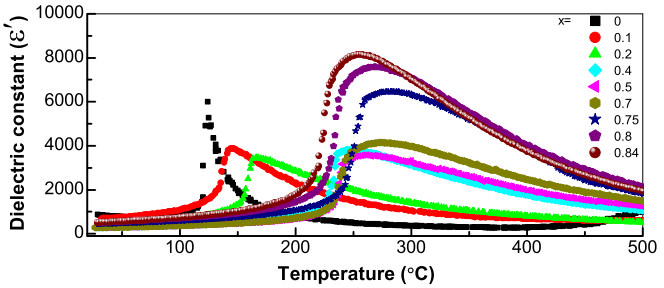

FIG. 1. (Color online) Temperature dependence of dielectric permittivity of $(1-x)$BT-(x)NBT measured at 10 kHz.

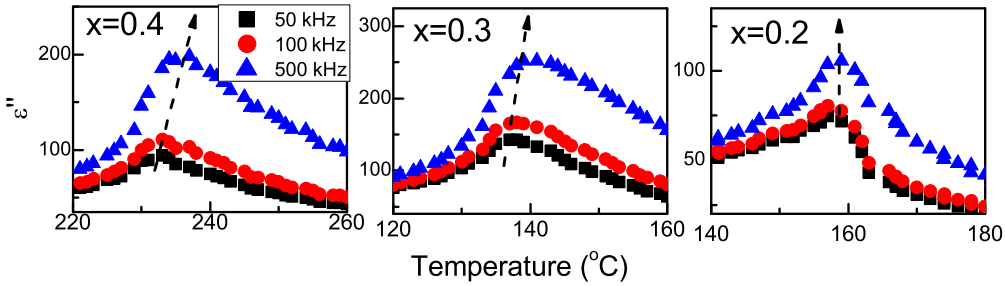

FIG. 2. (Color online) Frequency dispersion in temperature dependence of the imaginary part of the dielectric permittivity for three representative compositions of $(1-x)$BT-(x)NBT: $x = 0.2$, 0.3, and 0.4.

as shown in Fig. 2 for three representative compositions. Figure 3 shows the difference in the dielectric maximum temperatures of the imaginary part measured at 100 Hz and 10 kHz, i.e., $\Delta T_m'' = T_m''(10\,\text{kHz}) - T_m''(100\,\text{Hz})$ as a function of composition. $\Delta T_m''$ is zero up to $x = 0.20$ and then increases with increasing composition, thereby suggesting an increasing degree of polar relaxation with composition. Interestingly, this crossover from the normal to the diffuse/relaxor transition is accompanied by an abrupt jump in the anomaly temperature. Normal to relaxor crossover in modified BT has been investigated in different chemically modified BT such as Zr, Sn, and Sr [41,42]. The main difference to be noted is that while alloying with Sr, Zr, and Sn decreases the tetragonal-cubic dielectric anomaly temperature as well as the tetragonality $(c/a - 1)$, the opposite is the trend with $(Na_{0.5}Bi_{0.5})$. Figure 4 shows the temperature variation of the pseudocubic $\{200\}_c$ Bragg reflection for different compositions. A distinct increase in the tetragonal-cubic transition temperature can be noted when the composition increased from $x = 0.3$ to $x = 0.4$. This observation corresponds well with the composition variation of tetragonality at room temperature, which also shows a sudden increase in the tetragonality on going from $x = 0.3$ to $x = 0.40$ [Fig. 5(a)]. The enhanced tetragonality and dielectric anomaly temperature with increasing $(Na_{1/2}Bi_{1/2})$ content indicates that although chemical disorder drives the system towards the relaxor state, the local ferroelectric distortions is strengthened. The increase in the remnant polarization with increasing NBT concentration (not shown here) supports this view. X-ray diffraction studies have shown that the tetragonality $(c/a - 1)$ continues to increase with increasing NBT concentration and reaches a maximum of ~2% at $x = 0.80$. Table I shows the refined structural parameters of BT and 0.8NBT − 0.2BT obtained by Rietveld analysis of neutron powder diffraction data. It may be noted that a recent high resolution synchrotron x-ray powder diffraction study of BT has shown the presence of a subtle monoclinic phase coexisting with the tetragonal phase at room temperature [43]. However, for all practical purposes, due to the limitation associated with the resolution of neutron and laboratory x-ray powder diffractometers, the monoclinic phase can be treated as tetragonal. In view of this, in the present paper we have therefore considered the conventional tetragonal $(P4mm)$ structure for pure BT. It is interesting to note that cell volume has decreased from 65.03 Å^3 for BT to 62.04 Å^3 for 0.8NBT − 0.2BT. This decrease should be anticipated since the average radius of $Na_{1/2}Bi_{1/2}$ is 1.28 Å (Shannon radii of Na^{+1}, Bi^{+2} are 1.39 Å, 1.17 Å, respectively [44]) and is significantly less than that of Ba^{+2} (Shannon radius = 1.61 Å). Most important, however, is that this volume decrease is not isotropic as the tetragonality $c/a - 1$ gets doubled (from 0.01 for $x = 0$ to 0.02 for $x = 0.8$).

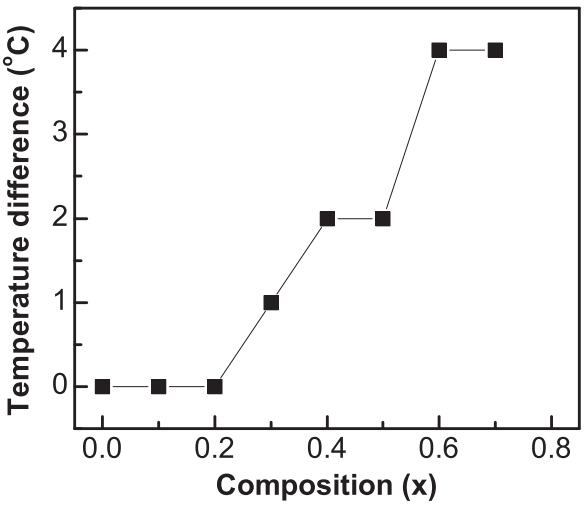

FIG. 3. Temperature difference between the dielectric anomaly of the imaginary part at 10 kHz and 100 kHz as a function of composition in $(1-x)$BT-(x)NBT.

B. Onset of long-period structural modulation and anomalous change in properties

As evident from Fig. 5(a), the tetragonality $c/a - 1$ of $(1-x)$ $BaTiO_3$-$(x)Na_{1/2}Bi_{1/2}TiO_3$ exhibits a maximum of 2% around $x = 0.80$ and then decreases very sharply with further increase in the NBT content. The same trend is observed in the composition dependence of the coercive field [Fig. 5(b)]. Both these observations suggest that though the structure remains tetragonal, there appears to be a qualitative change in the nature of interactions for $x > 0.8$. The clue to the subtle difference between the tetragonal phases across $x = 0.80$ was found from the neutron diffraction study. Figure 6 shows a vertically zoomed powder neutron diffraction pattern of $(1-x)$BT-(x)NBT in a limited 2θ range. The pattern of $x > 0.80$ shows weak superlattice reflections (marked by asterisks) in the angular range 35−39°. For $x < 0.80$, the superlattice reflections are not visible. Based on TEM studies, Ma *et al.* [35]

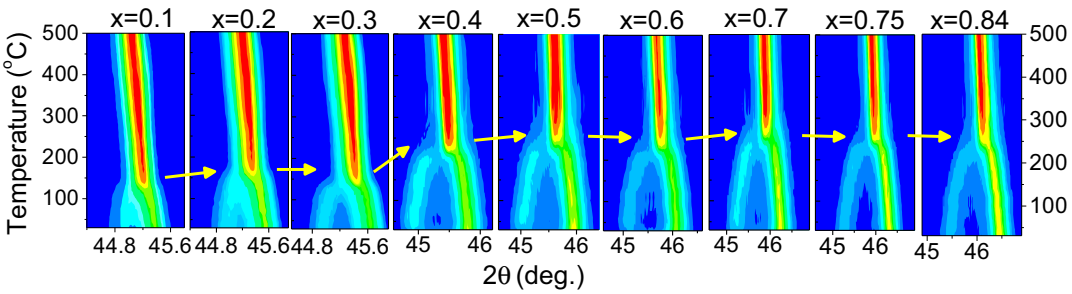

FIG. 4. (Color online) Graphical view of the temperature dependence of the (200)/(002) tetragonal Bragg profile of $(1-x)$BT-(x)NBT. The arrows mark the tetragonal-cubic transition.

have proposed an $R3c + P4bm$ phase coexistence for $0.94 < x < 0.95$, $P4bm$ for $0.90 < x < 0.94$, $P4bm + P4mm$ for $0.89 < x < 0.90$, and $P4mm$ for $x < 0.89$. Accordingly, we attempted to fit the neutron diffraction pattern of $x = 0.90$ with the $P4bm$ model [Fig. 7(a)]. However, this model fails to account accurately for the intensity and the positions of the observed superlattice peaks. In the angular range $35-39^\circ$, the $P4bm$ model predicts only one superlattice peak at $2\theta = 36.6^\circ$. Additional peaks marked by arrows remain unaccounted for by this structural model. It may be pointed out that since the main Bragg peaks of $x = 0.90$ can be explained by one set of tetragonal lattice parameters, there was no need to consider another phase to account for the superlattice peaks. In the next step, we attempted to index all the peaks by considering a doubled tetragonal cell $2a_t \times 2a_t \times 2c_t$ by Le Bail fitting. This also did not work, as shown in Fig. 7(b) by arrows for the unfitted portions of the superlattice reflections. The insufficiency of the $2 \times 2 \times 2$ supercell to index the superlattice reflections further indicates that the origin of these superlattice reflections cannot be explained in terms of the simple Glazer tilt system [45]. Inevitably, the superlattice reflections owe their origin to octahedral tilt configuration with a higher period modulation. Prosandeev *et al.* [46] have recently shown the propensity of perovskite structures to form modulated structures of the $\sqrt{2} \times \sqrt{2} \times n$, where n is the periodicity. The $P4bm$ cell belongs to this category with $n = 1$. The orthorhombic ($Pbnm$) cell of $CaTiO_3$ has $n = 2$. Because of the simplicity of this approach, we attempted to index the superlattice peaks in the neutron diffraction patterns with the $\sqrt{2}a_t \times \sqrt{2}a_t \times nc_t$ type cell. Since, as shown in Fig. 7(b), the $2 \times 2 \times 2$ cell is not sufficient, the $n = 2$ modulation was not tried. We also consistently noted that the odd number modulations were giving inferior fits compared to the immediate even numbered modulation. Hence, only the fits with even numbered n are shown in Figs. 7(c)–7(f). The minimum n required to obtain satisfactory fitting of the superlattice peaks was found to be 10. The superlattice reflections are not visible for $x < 0.80$. Thus within the tetragonal composition regime, $x = 0.80$ turns out to be the critical composition that separates a long period modulated tetragonal structure ($x > 0.80$) from a nonmodulated tetragonal structure ($x < 0.80$). The nonmodulated tetragonal structure is identical to that of BT. As shown above, it is this very critical composition below which the tetragonality and the coercive field drop sharply (Fig. 5). This clearly points out a relationship between the decrease in tetragonality and onset of long period structural modulation on the oxygen sublattice of the perovskite structure. The onset of this long range structural modulation also has direct bearing on the shape of the temperature dependence of the permittivity (ε') (Fig. 8). While for $x = 0.90$, the $\varepsilon'(T)$ shows two anomalies characterized by an abrupt jump at $T_d \sim 180\,^\circ$C followed by a broad maximum at $T_m \sim 250\,^\circ$C, for $x \leqslant 0.80$, $\varepsilon'(T)$ exhibits only one diffuse anomaly. The shape of the $\varepsilon'(T)$ plot of $x = 0.90$ is similar to that of pure NBT, in which case T_d is often referred to as the depolarization temperature.

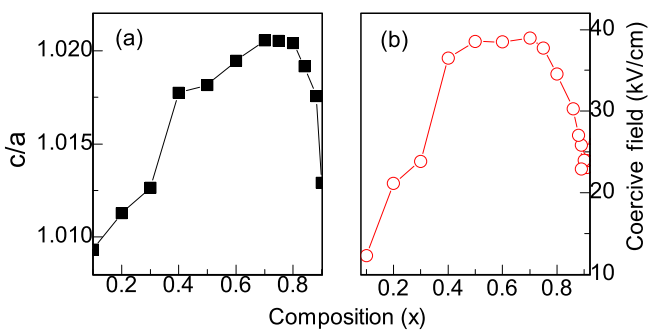

FIG. 5. (Color online) Composition dependence of (a) tetragonality c/a and (b) coercive field of $(1-x)$BT-(x)NBT.

IV. DISCUSSION

A. Normal-relaxor crossover

The relaxor state in a system exhibiting normal ferroelectricity can be induced by chemical disorder or pressure [47]. The chemical disorder already exists in the classical relaxor ferroelectric compound PMN. In the lead-free category, $Ba(Ti_{1-x}Zr_x)O_3$ (BTZ) is considered as one of the model relaxor ferroelectric systems. In comparison to PMN, the relaxor ferroelectric behavior of BTZ has been reported to exhibit several peculiarities such as (i) the pressure evolution of Raman spectra following the behavior of classical ferroelectrics and not of the classical relaxor ferroelectrics [48], (ii) dipolar dynamics neither following critical slowing down nor freezing into a glassy state below the diffuse dielectric anomaly temperature [49,50], (iii) absence of heat capacity anomaly [51], and (iv) persistence of the same correlation length of the polar regions in the relaxor compositions as in the compositions exhibiting normal ferroelectric behavior [52]. Recent first principles based effective Hamiltonian

TABLE I. Refined tetragonal ($P4mm$) structural parameters of $BaTiO_3$ and $0.2BaTiO_3-0.8$NBT using neutron powder diffraction data. The cation-anion distances are also shown in the bottom table

0.2BT-0.8NBT	x	y	z	U^{11} Å^2	U^{22} Å^2	U^{33} Å^2
Bi/Na/Ba	0.00000	0.00000	0.00000	0.0344 (10)	0.0344 (10)	0.0220 (17)
Ti	0.50000	0.50000	0.5653 (13)	0.0107 (7)	0.0107 (7)	0.0107 (7)
O1	0.50000	0.50000	0.0876 (9)	0.0164 (11)	0.0164 (11)	0.037 (2)
O2	0.50000	0.00000	0.5099 (11)	0.0212 (12)	0.0046 (9)	0.0162 (10)
$A = 3.90931(8)$ Å; $c = 3.98435(15)$ Å; vol $= 62.04$ Å^3						
R_p : 3.52; R_{wp} : 4.54; R_{exp} : 2.43; Chi^2 : 3.5						
$BaTiO_3$	x	y	z	U^{11} Å^2	U^{22} Å^2	U^{33} Å^2
Ba	0.00000	0.00000	0.00000	0.0065(5)	0.0065(5)	0.004(6)
Ti	0.50000	0.50000	0.506(12)	0.0123(7)	0.0123(7)	0.028(10)
O1	0.50000	0.50000	0.036(4)	0.0088(7)	0.0088(7)	0.011(3)
O2	0.50000	0.00000	0.529(4)	0.0084(7)	0.0098(6)	0.0062(6)
$A = 3.99388(6)$ Å; $c = 4.03538(7)$ Å; vol $= 65.03$ Å^3						
R_p : 4.48; R_{wp} : 5.72; R_{exp} : 2.18; Chi^2 : 6.88						

Bond-Length	No. of bonds	0.2BT-0.8NBT	$BaTiO_3$
Bi/Na/Ba-O1	4	2.7818	2.8278
Bi/Na/Ba-O2	4	2.7712	2.7569
Bi/Na/Ba-O3	4	2.8110	2.9231
Ti-O1	1	1.9611	1.8966
Ti-O2	1	2.0233	2.1388
Ti-O3	4	1.9709	1.9991

calculations have shown the polar nanoregions in BTZ to be centered around the Ti site. The Zr site possesses insignificant dipole moments [27,28]. This behavior may be representative of chemical disorder brought about by all isovalent substitutions at the Ti site in BT. For the chemical disorder at the A site, such as in $Ba_{1-x}Sr_xTiO_3$ (BST), the Ti sublattice is unaffected. The relaxor behavior in this system would arise from random local strain. Tiwari *et al.* [29] have shown the onset of diffuse transition in BST for $x \geqslant 0.12$. However, as in the present case, even for $x = 0.20$, the real part of the dielectric anomaly temperature of BST does not show noticeable frequency dependence. The frequency dependence of the anomaly temperature was captured in the imaginary part [29]. Interestingly, several groups have reported the persistence of the sharp dielectric anomalies in the real part in BST even for high x content [53–56]. Ostapchuk *et al.* [57] have reported ferroelectric transition even for $x\sim0.90$. Local structure analysis has revealed the existence of off-centered Ti ions and correlated displacements in BST for $x \geqslant 0.50$ [58,59]. This is surprising in the sense that for $x = 0.7$, BT is rather a minority component. The majority component, $SrTiO_3$, on the other hand is a paraelectric. The fact that modification of the A site with equimolar substitution of Na and Bi did not yield well developed features of relaxor ferroelectric even up to 70 mole percent of $Na_{1/2}Bi_{1/2}$ is very much analogous to the situation in BST. These results, in conjunction with the recent theoretical studies [27,28], suggest that the efficient way to achieve a well developed relaxor ferroelectric feature in stoichiometrically modified BT requires breaking of the Ti-Ti chemical correlation. Guided by the commonly observed trend, one of the viewpoints with regard to loss of long range polar coherence with increasing chemical disorder in modified BT based relaxor ferroelectric is associated with the weakening of the long range Coulombic interaction by substitution of nonferroelectric active ions. The loss of long range ferroelectric ordering in such systems is generally accompanied by a concomitant decrease in the tetragonality ($c/a - 1$). On the contrary, the $Na_{0.5}Bi_{0.5}$

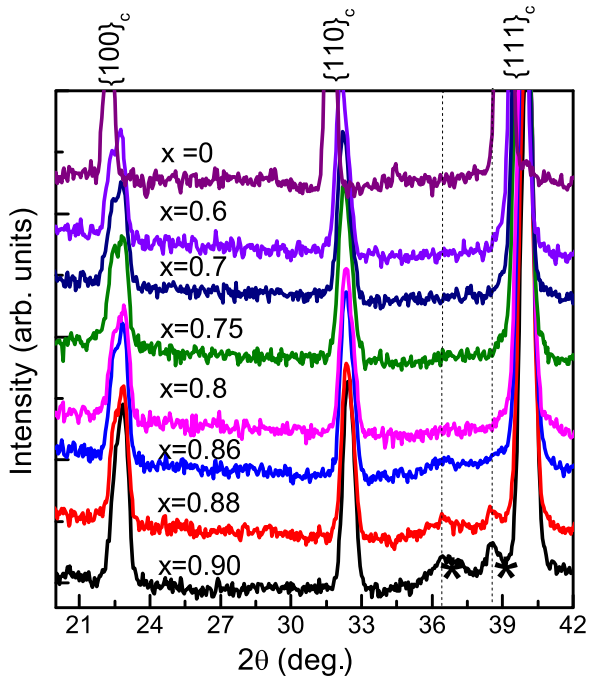

FIG. 6. (Color online) Part of the neutron powder diffraction pattern of $(1-x)$BT-(x)NBT. The small reflections marked with asterisks are superlattice reflections.

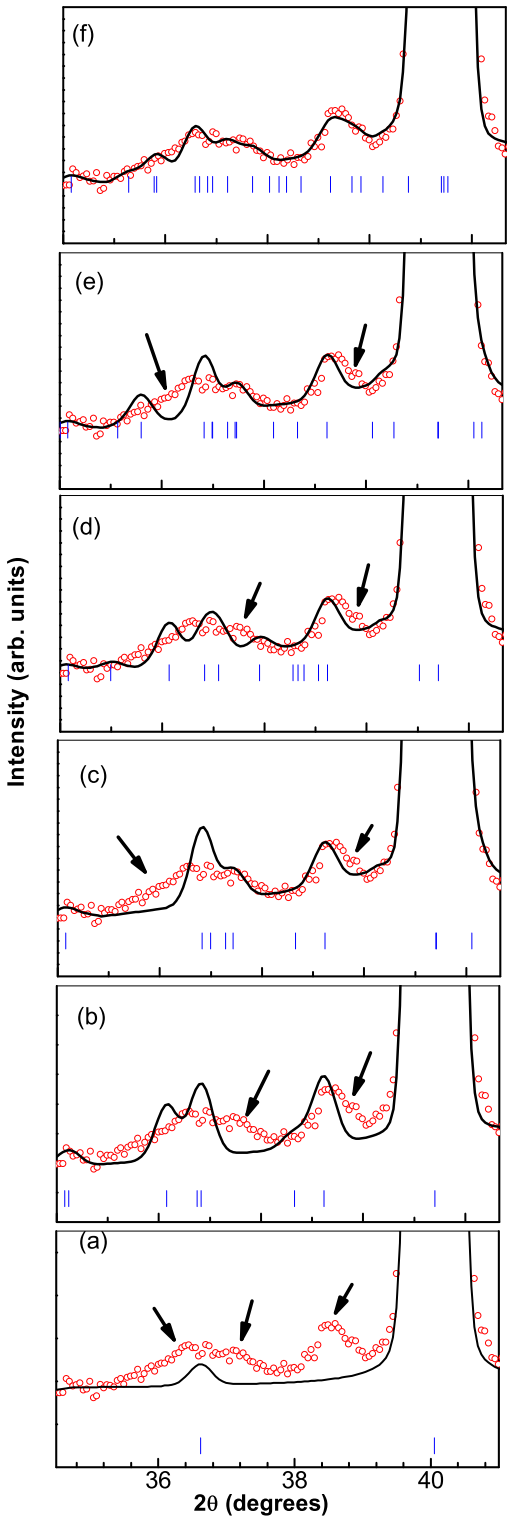

FIG. 7. (Color online) Rietveld fitted neutron powder diffraction pattern of 0.90NBT-0.10BT shown in a limited 2θ region near the observed superlattice reflections. The observed pattern is shown by open circles. The fitted patterns are shown by continuous lines. The unaccounted observed peaks are shown with arrows. Bragg peak positions are marked by vertical bars. Fitting was carried out by structural refinement using the $P4bm$ model (a), Le Bail fitting by a $2a_t \times 2b_t \times 2c_t$ cell (b). (c)–(f) Patterns are Le Bail fitted with a $\sqrt{2}a_t \times \sqrt{2}b_t \times nc_t$ type cell with $n = 4$ (c), $n = 6$ (d), $n = 8$ (e), and $n = 10$ (f).

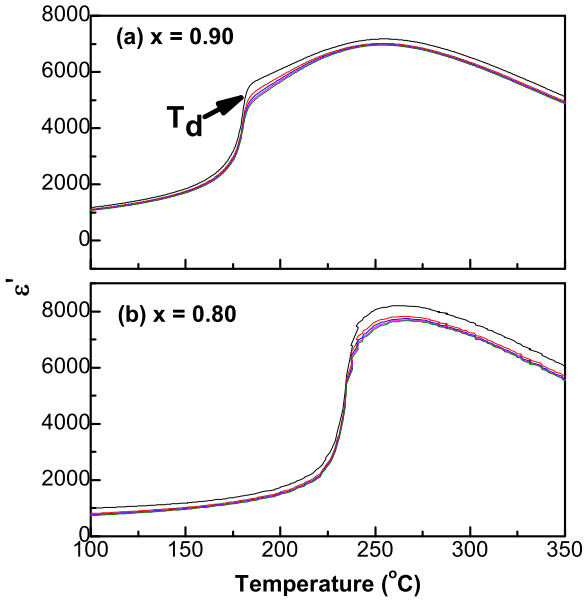

FIG. 8. (Color online) Temperature dependence of relative permittivity of $(1-x)$BT-(x)NBT for (a) $x = 0.90$ and (b) $x = 0.80$.

modified BT exhibits a tetragonality that is doubled (2%) as compared to BT (1%) for 0.8NBT − 0.2BT. At the same time, the atomic displacement parameters of 0.8NBT − 0.2BT is also significantly increased by approximately eightfold for the A site cations Na/Bi/Ba, suggesting that the enhanced tetragonality is accompanied by increased positional disorder, as expected for a relaxor system. Further, an important difference between Sr and Na/Bi modified BT is related to the fact that $Na_{0.5}Bi_{0.5}$ substitution makes the tetragonal phase the ground state [39], while Sr modification retains the rhombohedral ground state of BT [53–56]. The increase in the tetragonality can be understood by invoking the special role of the $6s^2$ lone pair electron of the Bi^{+3} ion, which is isoelectronic with Pb^{+2}. Cohen [60] has shown that the rhombohedral ground state of BT is determined primarily by the covalent interaction between Ti-3d and O-2p. On the other hand, in $PbTiO_3$ there is strong hybridization between the Pb and the O states, leading to a large strain that stabilizes the tetragonal ground state. Bi^{+3}, being isoelectronic with Pb^{+2}, is likely to increase the average covalent character of the A-O bond when substituted at the Ba site, thereby stabilizing the tetragonal phase as the ground state. As pointed out in the previous section, the substitution of the smaller size $Na_{1/2}Bi_{1/2}$ at the Ba site, although it decreases the volume of the unit cell, it does not change the bond distances isotropically. One important consequence of the strong anisotropic change is that it manifests as an overall increase in the tetragonality in the smaller volume cell. As can be seen from Table I, the A-O3 bond length decreases substantially from 2.92 Å to 2.81 Å as the NBT concentration increased to 80 mol. This particular shortening of the A-O bond distance is proof of its increased covalent character, which, in agreement with the first principles result [60], also helps in enhancing the tetragonality and stabilization of the tetragonal phase as the ground state [39].

B. Long-period modulation

The onset of a long-period modulation leading to abrupt decrease in the coercive field and tetragonality in this system for $x = 0.8$ is an interesting finding of this paper. The long-period modulation has earlier been shown for the cubiclike critical composition $x = 0.94$, which exhibits an anomalous piezoelectric response [38]. Occurrence of a long period (~60 Å) was first reported by Balagurov *et al.* [9] in pure NBT crystal by neutron diffuse scattering study. It appears that the coherence length of the long-period modulation is less in pure NBT, and Ba substitution seems to increase this coherence length as a result of which distinct superlattice reflections corresponding to the long-period modulation become visible in the neutron diffraction patterns of NBT-BT. Interestingly enough, though diffuse scattering has also been reported in electron diffraction studies, such studies have not reported long range modulation in the NBT-BT series. As per the phase diagram of Ma *et al* [35]. based on TEM studies, $x = 0.94$ is described in terms of the coexistence of $R3c$ and $P4bm$ phases. It is, however, important to bear in mind that the XRD pattern of this composition does not require two different sets of lattice parameters, corresponding to two of the different phases to account for the fundamental Bragg peaks. In fact, two phases led to nonconvergence of the Rietveld refinement, confirming that the Bragg peaks can be fitted exactly with a cubic lattice parameter for $x = 0.94$ [38]. In view of this, it is therefore important to relate the superlattice reflections as arising from modulation of the cubiclike primitive cell. The same scenario exists for tetragonal compositions with $x > 0.80$. With the present data, we have not attempted to resolve the accurate structural model for the modulated phases since the intensity of the superlattice peaks are very small and are overlapping, giving the impression that the superlattice reflections possess a larger width than the main Bragg reflections. Better resolution data with better counting statistics would be desirable for reliable structural analysis of the modulated phases. Complex octahedral tilt with long-period modulations have been reported for different perovskite systems such as $NaNbO_3$ [61,62], $(Ca,Sr)TiO_3$ [63], and $BiFeO_3$ [46,64]. Prosandeev *et al.* [46] have theoretically predicted different complex modulated phases in perovskite structure resulting from coupling between electric dipoles and antiferrodistortive distortions associated with octahedral tilts. A universal collaborative coupling between oxygen octahedral rotations and antiferroelectric distortions in perovskites has been argued [65]. Antiferroelectric correlation has been reported to play an important role in the anomalous behavior of relaxor ferroelectrics and high performance piezoelectrics [66–68]. A collaborative coupling between antiphase, in-phase octahedral tilts and antipolar cationic displacements is known to occur in orthorhombic ($Pbnm$) perovskites, e.g., $CaTiO_3$. This structure exhibits an $a^-a^-c^+$ octahedral tilt. The long-period modulated phases in $BiFeO_3$ predicted by Prosandeev *et al.* [64] are considered as the bridge between rhombohedral $R3c$ and the $Pbnm$ distortions. While the $R3c$ phase is ferroelectric in nature, the $Pbnm$ phase is not so. Though, using electron diffraction studies, Dorcet *et al.* [69] have proposed the stabilization of the $Pbnm$ phase in NBT at ~300 °C, the bulk diffraction techniques have revealed a cubiclike lattice with pronounced in-phase ($a^0a^0c^+$) octahedral tilt [34]. This transition has also been characterized as an isotropization temperature by some groups [16,70]. In principle, the modulated phase can be either antiferroelectric or ferroelectric depending on whether the modulated cell is centrosymmetric or not. The long-period modulated phases in $NaNbO_3$, $(Sr, Ca)TiO_3$, and $PbZrO_3$ show centrosymmetric structures and hence are antiferroelectrics. Tagantsev *et al.* [71] have described antiferroelectrics as a missed incommensurate phase. The complex tilt configuration in NBT-BT appears to be a result of competing $a^-a^-a^-$ and $a^0a^0c^+$ tilt modes. High temperature XRD and neutron diffraction studies have revealed that the superlattice reflections characteristic of the long range octahedral modulation appear at a significantly higher temperature than the depolarization temperature [34]. Hence, the polarization degree of freedom is not involved in the formation of the long-period modulated phase in this system. At the same time, the framework of long-period modulation precludes the development of long coherence of polarization and drives the system towards a relaxor state [34]. Datta *et al.* [72] have shown that the critical composition exhibits strong softening and damping of phonon modes related to vibrations of the Na/Bi and the Ti ions at the tricritical point temperature. This enhanced damping is likely to be linked with the development of ferroelectric correlation in the matrix of the long-period modulated structure.

V. CONCLUSIONS

The lead-free piezoelectric $Na_{1/2}Bi_{1/2}TiO_3$-$BaTiO_3$ is shown to exhibit a rich variety of phenomena across the entire composition range. Near the BT end, the system exhibits a crossover from a normal to a diffuse/relaxor transition. However, unlike other chemical modifications of BT reported in the past (Zr, Sn, Sr, etc.) where the relaxor state is accompanied by a weakening of ferroelectric distortion and a decrease in the critical temperature, the onset of the relaxor state by $Na_{1/2}Bi_{1/2}$ substitution on the Ba site increases the spontaneous tetragonal strain due to enhancement in the covalent character of the A-O bond by virtue of the Bi^{+3} $6s^2$ lone pair effect. We also demonstrate evidence of a new criticality at $x = 0.8$ where the electrical coercivity and the spontaneous tetragonal strain exhibit a nonmonotonic dependence with composition. Neutron diffraction study revealed this new criticality to be associated with the crossover from a nonmodulated tetragonal phase (for $x < 0.8$) to a long-period modulated tetragonal phase (for $x > 0.8$). The existence of the long-period modulated state is shown to depolarize the system well before the diffuse dielectric anomaly temperature. In contrast to the often reported two-phase state for the critical compositions for this system, our results offer a new perspective with regard to the structure-property correlation in this system and is consistent with some of the recent theoretical predictions.

ACKNOWLEDGMENTS

R.R. acknowledges the Science and Engineering Board (SERB) of the Department of Science and Technology, Government of India, for financial assistance provided by Grant No. SERB/F/5046/2013-14.

[1] S.-T. Zhang, A. B. Kounga, E. Aulbach, H. Ehrenberg, and J. Rödel, Appl. Phys. Lett. **91**, 112906 (2007).

[2] W. Jo, T. Granzow, E. Aulbach, J. Rödel, and D. Damjanovic, J. Appl. Phys. **105**, 094102 (2009).

[3] J. Rödel, W. Jo, K. T. P. Seifert, E.-M. Anton, T. Granzow, and D. Damjanovic, J. Am. Ceram. Soc. **92**, 1153 (2009).

[4] C.-S. Tu, I. G. Siny, and V. H. Schmidt, Phys Rev. B **49**, 11550 (1994).

[5] B. N. Rao, R. Datta, S. S. Chandrashekaran, D. K. Mishra, V. Sathe, A. Senyshyn, and R. Ranjan, Phys. Rev. B **88**, 224103 (2013).

[6] M. Matsura, H. Ida, K. Horita, K. Ohwada, Y. Noguchi, and M. Miyayama, Phys. Rev B **87**, 064109 (2013).

[7] J. Petzelt, D. Nuzhnyy, V. Bovtun, M. Kempa, M. Savinov, S. Kamba, and J. Hlinka, Phase Trans. **88**, 320 (2014).

[8] G. O. Jones and P. A. Thomas, Acta Crystallogr. B **58**, 168 (2002).

[9] A. M. Balagurov, E. Y. Koroleva, A. A. Naberezhnov, V. P. Sakhnenko, B. N. Savenko, N. V. Ter-Oganessian, and S. B. Vakhrushev, Phase Trans. **79**, 163 (2007).

[10] J. Petzelt, S. Kamba, J. Fabry, D. Noujni, V. Porokhonskyy, A. Pashkin, I. Franke, K. Roleder, J. Suchanicz, R. Klein, and G. E. Kugel, J. Phys. Condens. Matter **16**, 2719 (2004).

[11] I. Levin and I. M. Reaney, Adv. Funct. Mater. **22**, 3445 (2012).

[12] M. Groting, S. Hayn, and K. Albe, J. Solid State Chem. **184**, 2041 (2011).

[13] M. Groting, I. Kornev, B. Dkhil, and K. Albe, Phys. Rev. B **86**, 134118 (2012).

[14] B. N. Rao, A. N. Fitch, and R. Ranjan, Phys. Rev. B **87**, 060102 (2013).

[15] B. N. Rao and R. Ranjan, Phys. Rev. B **86**, 134103 (2012).

[16] S. Gorfman and P. A. Thomas, J. Appl. Crystallogr. **43**, 1409 (2010).

[17] E. Aksel, J. S. Forrester, J. L. Jones, P. A. Thomas, K. Page, and M. R. Suchomel, Appl. Phys. Lett. **98**, 152901 (2011).

[18] R. Beanland and P. A. Thomas, Phys. Rev. B **89**, 174102 (2014)

[19] J. Kreisel, A. M. Glazer, P. Bouvier, and G. Lucazeau, Phys. Rev. B **63**, 174106 (2001).

[20] D. S. Keeble, E. R. Barney, D. A. Keen, M. G. Tucker, J. Kreisel, and P. A. Thomas, Adv. Funct. Mater. **23**, 185 (2013).

[21] E. Aksel, J. S. Forrester, J. C. Nino, K. Page, D. P. Shoemaker, and J. L. Jacob, Phys. Rev. B **87**, 104113 (2013).

[22] V. A. Shuvaeva, D. Zekria, A. M. Glazer, Q. Zhang, S. M. Weber, P. Bhattacharya, and P. A. Thomas, Phys. Rev. B **71**, 174114 (2005).

[23] V. Dorcet and G. Trolliard, Acta Mater. **56**, 1753 (2008).

[24] R. Comes, M. Lambert, and A. Guinier, SSC **6**, 715 (1968); M. Lambert and R. Comes, *ibid.* **7**, 305 (1969).

[25] J. Harada, M. Watanabe, S. Kodera, and G. Honjo, J. Phys. Soc. Jpn. **20**, 630 (1965).

[26] Y. Liu, R. L. Withers, B. Nguyen, and K. Elliott, Appl. Phys. Lett. **91**, 152907 (2007).

[27] A. R. Akbarzadeh, S. Prosandeev, E. J. Walter, A. Al-Barakaty, and L. Bellaiche, Phys. Rev. Lett. **108**, 257601 (2012).

[28] S. Prosandeev, D. Wang, and L. Bellaiche, Phys. Rev. Lett. **111**, 247602 (2013).

[29] V. S. Tiwari, N. Singh, and D. Pandey, J. Phys. Condens. Matter **7**, 1441 (1995).

[30] V. Westphal, W. Kleeman, and M. D. Glinchuk, Phys. Rev. Lett. **68**, 847 (1992).

[31] A. A. Bokov and Z.-G. Ye, J. Mat. Sc. **41**, 31 (2006).

[32] F. Cordero, F. Cracium, F. Trequattrini, E. Mercadelli, and C. Galassi, Phys. Rev. B **81**, 144124 (2010).

[33] W. Jo, J. E. Daniels, J. L. Jones, X. Tan, P. A. Thomas, D. Damjanovic, and J. Rödel, J. Appl. Phys. **109**, 014110 (2011).

[34] R. Garg, B. N. Rao, A. Senyshyn, P. S. R. Krishna, and R. Ranjan, Phys. Rev. B **88**, 014103 (2013).

[35] C. Ma, H. Guo, and X. Tan, Adv. Funct. Mater. **23**, 5261 (2013).

[36] T. Takenaka, K. Maruyama, and K. Sakata, Jpn. J. Appl. Phys. **30**, 2236 (1991).

[37] R. Ranjan and A. Dviwedi, Solid State Commun. **135**, 394 (2005).

[38] R. Garg, A. Senyshyn, and R. Ranjan, J. Appl. Phys. **114**, 234102 (2013)

[39] K. Datta, P. A. Thomas, and K. Roleder, Phys. Rev. B **82**, 224105 (2010).

[40] J. Rodrigues-Carvajal, *FullProf. A Rietveld Refinement and Pattern Matching Analysis Program, Laboratoire Leon Brillouin (CEA-CNRS)* (France, 2000).

[41] T. Maiti, R. Guo, and A. S. Bhalla, Appl. Phys. Lett. **90**, 182901 (2007).

[42] J. Ravez and A. Simon, Eur. J. Solid State Inorg. Chem. **34**, 1199 (1997).

[43] A. K. Kalyani, D. K. Khatua, B. Loukya, R. Datta, A. N. Fitch, A. Senyshyn, and R. Ranjan, Phys. Rev. B **91**, 104104 (2015).

[44] R. D. Shannon, Acta. Cryst. A **32**, 751 (1976).

[45] A. M. Glazer, Acta. Cryst. A **31**, 756 (1975).

[46] S. Prosandeev, D. Wang, W. Ren, J. Iniguez, and L. Bellaiche, Adv. Funct. Mater. **23**, 234 (2013).

[47] G. A. Samara, J. Phys. Condens. Matter **15**, R367 (2003).

[48] J. Kreisel, P. Bouvier, M. Maglione, B. Dkhil, and A. Simon, Phys. Rev. B. **69**, 092104 (2004).

[49] A. A. Bokov, M. Maglione, and Z. G. Ye, J. Phys. Condens. Matter **19**, 092001 (2007).

[50] S. Ke, H. Fan, H. Huang, H. L. W. Chan, and S. Yu, J. Appl. Phys. **104**, 034108 (2008).

[51] M. Nagasawa, H. Kawaji, T. Tojo, and T. Atake, Phys. Rev. B **74**, 132101 (2006).

[52] S. Miao, J. Pokorny, U. M. Pasha, O. P. Thakur, D. C. Sinclair, and M. Reaney, J. Appl. Phys **106**, 114111 (2009).

[53] V. V. Lemanov, E. P. Smirnova, P. P. Syrnikov, and E. A. Tarakanov, Phys. Rev. B **54**, 3151 (1996).

[54] V. B. Shirokov, V. I. Torgashev, A. A. Barkirov, and V. V. Lemanov, Phys. Rev. B **73**, 104116 (2006).

[55] T. Ostapchuk, J. Petzelt, J. Hlinka, V. Bovtun, P. Kuzel, I. Ponomareva, S. Lisenkov, L. Bellaiche, A. Tkach, and P. Vilarinho, J. Phys. Condens. Matter **21**, 474215 (2009).

[56] O. G. Vendik, E. K. Hollman, A. B. Kozyrev, and A. M. Prudan, J. Supercond. **12**, 325 (1999).

[57] T. Ostapchuk, M. Savinov, J. Petzelt, A. Pashkin, M. Dressel, E. Smirnova, V. Lemanov, A. Sotnikov, and M. Weihnacht, Ferroelectrics, **353**, 70 (2007).

[58] V. Shuevaeva, Y. Azuma, K. Yagi, H. Terauchi, R. Vedrinski, V. Komarov, and H. Kasatani, Phys. Rev. B, **62**, 2969 (2000).

[59] I. Levin, V. Krayzman, and J. C. Woicik, Phys. Rev. B **89**, 024106 (2014).

[60] R. E. Cohen, Nature **358**, 136 (1992).

[61] M. D. Peel, S. P. Thompson, A. D. Aladine, S. E. Ashbrook, and P. Lightfoot, Inorg. Chem. **51**, 6876 (2012).

[62] S. K. Mishra, R. Mittal, V. Y. Pomjakushin, and S. L. Chaplot, Phys. Rev. B **83**, 134105 (2011).
[63] R. Ranjan, D. Pandey, and N. P. Lalla, Phys. Rev. Lett. **84**, 3726 (2000).
[64] S. A. Prosandeev, D. D. Khalyavin, I. P. Raevski, A. N. Slak, N. M. Olekhnovich, A. V. Pushkarev, and Y. V. Radyush, Phys. Rev. B **90**, 054110 (2014).
[65] L. Bellaiche and J. Iniguez, Phys. Rev. B **88**, 014104 (2013).
[66] J. Hlinka, P. Ondrejkvic, M. Kempa, E. Borissenko, M. Krisch, X. Long, and Z.-G. Ye, Phys. Rev. B **83**, 140101(R) (2011).
[67] S. A. Prosandeev, M. S. Panchelyuga, S. I. Raevskaya, and I. P. Raevskii, Phys. Solid State **53**, 147 (2011).
[68] I. Grinberg, V. R. Cooper, and A. M. Rappe, Phys. Rev. B, **69**, 144118 (2004).
[69] V. Dorcet, G. Trolliard, and P. Boullay, Chem. Mater. **20**, 5061 (2008).
[70] M. Geday, J. Kreisel, A. M. Glazer, and K. Roleder, J. Appl. Crystallogr. **33**, 909 (2000).
[71] A. K. Tagantsev, K. Vaideeswaran, S. B. Vakhrushev, A. V. Filimonov, R. G. Burkovsky, A. Shaganov, D. Andronikova, A. I. Rudskoy, A. Q. R. Baron, H. Uchiyama, D. Chernyshov, A. Bosak, Z. Ujma, K. Roleder, A. Majchrowski, J.-H. Ko, and N. Setter, Nat. Comm. **4**, 2229 (2013).
[72] K. Datta, A. Richter, M. Gobbels, R. B. Neder, and B. Mihailova, Phys. Rev. B **90**, 064112 (2014).